Spalling behaviour of concrete made with recycled concrete aggregates

Bruno Fernandes, Hélène Carré, Jean-Christophe Mindeguia, Céline Perlot-Bascoules, Christian La Borderie

Version of Record: https://www.sciencedirect.com/science/article/pii/S0950061822017895
Manuscript_a1a08e4d2288f566386b7d1a96213646

Spalling behaviour of concrete made with recycled concrete aggregates

Bruno Fernandes[a], Hélène Carré[a], Jean-Christophe Mindeguia[b], Céline Perlot[a,c], Christian La Borderie[a]

[a] *Université de Pau et des Pays de l'Adour, E2S UPPA, SIAME, Anglet, France*
[b] *Université de Bordeaux, Laboratoire l2M, Talence, France*
[c] *Institut Universitaire de France (IUF)*

Abstract

Concrete made with recycled concrete aggregates (RCA) presents particular properties that may lead to a specific behaviour under fire conditions, including the spalling risk. The spalling sensitivity of concrete made with RCA was evaluated through a campaign conducted in three concrete series: reference, direct replacement, and strength-based replacement. The last was designed to have the same performance as concrete made with natural aggregates (NA). Samples with different replacement rates of recycled coarse aggregates (0 %, 10 %, 20 %, 40 %, and 100 %) were exposed to the standard fire curve (ISO 834-1) with constant uniaxial loading (2.5 and 5 MPa). During the tests, the furnace temperature and spalling events were recorded. After the tests, digital photogrammetry was used to observe the spalling damage (volume and depth). Fire tests indicated that concrete made with RCA exhibited a higher spalling degree than concrete made with NA. Results also show that the replacement rate acts in different ways: in concrete with RCA replacement rates up to 40 %, the spalling damage increases, but a further increase does not lead to higher spalling. In addition, RCA changes the physical properties of concrete, which may trigger spalling, particularly water content.

Keywords:
Recycled concrete aggregates, spalling tests, spalling, screening tests, fire behaviour

Email address: bruno.fernandes@univ-pau.fr (Bruno Fernandes)

1. Introduction

One of the main concerns when evaluating the fire behaviour of concrete structures is spalling. This phenomenon consists of violent or nonviolent detachment of concrete fragments from the surface of a concrete member [1, 2]. Depending on the severity of the damage, fire spalling can seriously affect the structural performance because it reduces the cross section and may even expose steel rebars directly to the fire. This can lead to a reduction in fire resistance, thermal insulation, and load-bearing capacity [3–5]. Despite extensive research in recent years, uncertainties regarding the phenomenon remain, and current models cannot predict spalling events [4, 6, 7].

Concrete behaviour under fire is a coupled thermo-hygro-chemo-mechanical problem, and all these mechanisms can contribute to the spalling phenomenon [2]. Spalling is usually explained by one of two theories, (i) pore pressure build-up and (ii) thermal stresses, which may occur individually or jointly [2, 8]. The first, pore pressure build-up, is a thermo-hygral process driven by water vaporisation and transport. During heating, the vapour moves towards the exposed surface and into the inner part of the concrete (nonheated). Owing to thermal gradients, the vapour may condense in the inner core, creating a saturated layer a few centimetres from the exposed side (the so-called 'moisture clog'). This zone blocks further vapour movement, leading to an increase in pore pressure. When stresses resulting from pore pressure exceed the tensile strength of concrete, spalling may occur [2, 4, 9–11].

The second theory is a thermo-mechanical process driven by thermal-gradient-induced thermal stresses and/or restrained thermal dilation [2]. When these high stresses (compressive ones), localized in the first centimetres of the concrete surface, exceed concrete strength, spalling may occur [4, 8, 12]. Usually, spalling is also attributed to the coupled action of these mechanisms (thermo-hygral and thermo-mechanical), i.e., a combination of pore pressure, compression stresses (induced by thermal action and loading), and cracking [1]. One last mechanism, the thermo-chemical spalling, was also proposed, in which the phenomenon is related to the decomposition of calcium hydroxide and the rehydration of calcium oxide [2].

In addition to these theories, different mathematical and numerical models were developed to understand spalling and concrete behaviour at high temperatures [13]. These models, mainly based on hygro-thermo-mechanical mechanisms, are usually analysed with phenomenological [11, 14] or mechanistic approaches [15]. The complexity of the spalling problem is also

highlighted by the several parameters that may influence the occurrence of spalling. These parameters can be classified into material (e.g., permeability, porosity, and water content), geometry (e.g., shape and size of elements), and environmental (e.g., heating rate, heating profile, and external mechanical load) factors [1]. In addition, spalling can occur in different forms, such as aggregate, surface, explosive, and corner spalling [1, 12].

Little is known about the susceptibility of concrete made with recycled concrete aggregates (RCA) to spalling, and the prediction of its sensitivity to spalling is generally not trivial. On the one hand, because RCAs are more porous than natural aggregates (NA), the use of this type of aggregate may contribute to vapour migration, reducing the pore pressure and spalling risk [16]. On the other hand, RCAs have higher water absorption, which may lead to concrete with higher water content, i.e., a key parameter for spalling risk [17, 18]. Finally, more interfacial transition zones are observed in concrete made with RCA (old paste/new paste, old aggregate/new paste), which may lead to distinct behaviour under high temperatures.

Few studies have verified the occurrence of fire spalling in recycled concrete aggregate (RAC) [19]. Robert et al. [20] studied the spalling behaviour of concrete slabs made with RCA. They tested two reference slabs and two slabs of concrete made with RCA (one with 30 % coarse RCA and the other with 30 % both fine and coarse RCA). All the elements were tested under the ISO 834-1 [21] fire curve for 60 min. Superficial and localised spalling was observed in all slabs containing RCA, whereas slabs with NA did not exhibit any spalling. This phenomenon was attributed to the high moisture content of RAC slabs - between 4.4 % and 5.5 % at the element surface, whereas reference slabs had a moisture content of 4.0 %. However, the extent of damage in RAC slabs was not detrimental to their stability. Chen et al. [22] evaluated the mechanical properties of reinforced concrete and steel-reinforced concrete (i.e., composite) short columns and beams after exposure to elevated temperatures. Samples prepared with different replacement rates were heated in an electric furnace. Spalling in samples heated to 800 °C was reported, but no further details or explanations were provided

Spalling was also observed by Pliya et al. [16, 23]. In the first study [16], they tested the spalling sensitivity of high-strength concrete made with NA and RCA (0 %, 15 %, and 30 % replacement rates). Concrete cylinder samples were heated in an electric furnace at a rate of 10 °C/min. All mixes (with or without RCA) showed progressive and explosive spalling, characterised by the sudden disintegration of all samples. A similar phenomenon was observed

in another study [23], in which spalling was found in samples subjected to preloading and when the surface temperature reached 150 °C. For samples made with NA spalling happened at 450 °C.

The aforementioned experimental studies demonstrated that spalling can occur in concrete made with RCA. However, systematic evaluation of the spalling risk of concrete made with RCA has not been performed. This lack of information prevents the robust design of concrete made with RCA regarding its fire behaviour. In this study, the fire spalling sensitivity of concrete made with RCA was investigated experimentally. The purpose of this research was to conduct a material screening test to provide a qualitative and comparative evaluation of the spalling behaviour of concrete made with RCA.

Fire tests on uniaxially loaded samples were performed. Ordinary concrete mixes containing different replacement rates of coarse aggregates (10 %, 20 %, 40 %, and 100 %) were subjected to the ISO 834-1[21] fire curve. In addition to the replacement rate, the effect of the external mechanical load and replacement method were studied. Spalling events were registered during the fire tests. For postfire spalling assessment, a method based on digital photogrammetry was used. Finally, the spalling behaviour of the specimens and the influence of RCA were examined in light of common spalling theories.

2. Experimental program

2.1. Materials

Concrete mixes were prepared using cement CEM II/A-L 42.5R (Eqiom). This cement has a density of 3010 kg/m^3 and a specific surface area of 4700 cm^2/g. To achieve the desired workability, limestone filler (Omya Betocarb HP-SC) was used. This filler has a density of 2700 kg/m^3 and a specific surface area of 4330 cm^2/g. A polycarboxylate-based superplasticiser (SIKA ViscoCrete Tempo-483) was used in the mixes.

Alluvial sand with a fineness modulus of 3.10 was used. Two types of coarse aggregates were used: NA and RCA. Natural aggregates were made from diorite (Genouillac, France) and divided into two fractions: 4/10 and 10/20. The recycled concrete aggregates were crushed and screened by a recycling company near Bordeaux (France). They were divided into the same fractions as the NA. The physical properties (density, water absorption, and LA coefficient), measured according to EN 1097-2:2010 [24] and EN 1097-6:2013 [25], are presented in Table 1. As expected, RCA had higher water

absorption and a lower LA coefficient owing to the presence of the adhered mortar.

Table 1: Aggregate properties

Property	Sand	Natural aggregate		Recycled aggregate	
Grading size	0/4	4/10	10/20	4/10	10/20
Density (kg/m^3)	2650	2820	2840	2570	2590
Water absorption (%)	0.35	0.92	0.81	5.60	4.52
LA coefficient (%)	-	16	16	30	36

Because RCAs were obtained from a recycling plant, they also presented some impurities related to demolition wastes, such as wood, plastic, brick, and bituminous materials. To quantify these impurities, manual sorting was performed following EN 933-11:2009 [26] guidelines. The results of this classification are listed in Table 2.

Table 2: RCA constituents

Aggregate Fraction	Constituents (% of mass)*					
	Rc	Ru	Rb	Ra	Rg	X
RCA 4/10	73.31	23.97	0.53	2.14	-	0.05
RCA 10/20	76.77	18.59	0.50	3.87	0.07	0.19

*Rc: concrete grains, Ru: natural stones, Rb: ceramic elements, Ra: bituminous grains, Rg: glass, X: other materials (wood, plastic,steel, paper, etc.)

2.2. Mixture design and casting

To investigate the fire spalling behaviour of concrete made with RCA, a comprehensive test program was undertaken on seven mixes divided into three categories: reference, direct replacement (DR), and strength-based replacement (SBR). Table 3 presents the mixture proportions for all the mixes. The reference samples are concrete made with NA, designed to meet the NF EN 206/CN:2014 [27] durability requirements for the XD3 exposure class. This class determines a maximum water/cement (w/c) ratio of 0.5, a compressive strength class of C35/45, and a minimum cement content of 350 kg/m^3. In DR mixes, NA was replaced by RCA in volume without any changes in the other constituents. Replacement rates for this mix were chosen based on the RECYBETON [28] French project recommendations, which, for

XD3 exposure classes, allow maximum replacement rates of 20 % and 40 %. Additional replacement rates of 10 % and 100 % were also studied for the DR mixes.

In SBR mixes, in addition to aggregate replacement, the cement and water contents were adjusted to achieve the same strength as the reference mix. To adjust mixes, BetonLab [29] software was used. Based on the compressive strength results of the reference and DR mixes, the properties of the aggregates (p and q coefficients, which describe the aggregate contribution to the compressive strength) were calibrated. Then, new mixes were designed. The w/c ratio was adjusted to achieve the same compressive strength as that of the reference mix. The water and cement contents were adjusted to achieve the target consistency. For the SBR mixes, replacement rates of 40 % and 100 % were studied.

Table 3: Mix proportions (in kg/m^3, SP in percentage of cement mass)

Material	Mix						
	NA	RCA-10-DR	RCA-20-DR	RCA-40-DR	RCA-100-DR	RCA-40-SBR	RCA-100-SBR
Cement	350	350	350	350	350	368	420
Filler	60	60	60	60	60	60	60
Sand	804.3	804.3	804.3	804.3	804.3	787.1	799.8
NA 4/10	331.7	298.5	265.3	199.0	-	207.2	-
NA 10/20	711.1	640.0	568.9	426.7	-	447.5	-
RCA 4/10	-	30.2	60.5	120.9	302.3	114.7	291.5
RCA 10/20	-	64.9	129.7	259.4	648.5	248.1	630.3
Water	175	175	175	175	175	172	168
SP	0.9	0.9	0.9	0.9	0.9	0.9	0.9

One concern when using RCA stems from its higher water absorption. This property can affect the workability of concrete, even when moisture adjustments are made to the mixes [30]. To develop a method that can be easily reproduced in a concrete plant, all the aggregates (sand, NA, and RCA) were prewetted for 1 h using a soaker hose and then covered with a plastic sheet for 3 h. Before casting, the moisture content of the aggregates was measured and the water quantity of the mix was corrected.

Preliminary studies showed some variations in workability and compressive strength, even for the same mixes. Because the ratio between the slump and compressive strength was constant in the preliminary mixes, mixes with dried aggregates were cast to verify the reference slump and its corresponding compressive strength. These values were used as a reference for the final mixes (slump between 180 and 190 mm). In the final mixes, the aggregates were prewetted, and the water content was adjusted to achieve the same

slump as the reference. The same mixing procedure was used for all the concrete mixes. The slump was measured after mixing following NF EN 12350-2 [31].

For each mix, cylindrical specimens (11 x 22 cm and 16 x 32 cm) were cast to determine the mechanical properties at 28 days and at the fire test age. For the fire tests, prisms with dimensions of 20 x 20 x 10 cm (height x length x width) were cast. Except for the cylindrical samples used to determine the properties at 28 days, which were kept submerged in water at 20 °C until the testing day, the samples were first kept submerged for seven days and then placed in sealed plastic bags until test (between 88 and 125 days). This curing induced a high water content (when compared with air curing), thus inducing a high probability of spalling for all the mixes. At the test age, the water content (wc), density (ρd), and water-accessible porosity (η) were measured following the NF EN 12390-7:2019 [32] and AFREM recommendations [33]. The slump, mechanical and physical properties of all the studied mixes are listed in 4.

Table 4: Fresh, mechanical, and physical properties of studied mixes

Mix	Slump (mm)	f_{c28} (MPa)	j (days)	$f_{c,j}$ (MPa)	$E_{c,j}$ (GPa)	wc (%)	ρd (g/cm^3)	η (%)
NA	194	44.8	94	46.6	34.5	4.9	2.3	12.3
RCA-10-DR	184	39.7	116	44.5	36.8	5.0	2.2	13.8
RCA-20-DR	174	37.4	88	50.8	34.9	5.1	2.2	16.0
RCA-40-DR	176	39.7	88	49.6	39	5.4	2.2	15.2
RCA-100-DR	210	34.6	125	39.1	30.5	7.1	2.1	18.1
RCA-40-SBR	192	44.6	94	46.8	31.8	5.7	2.2	15.3
RCA-100-SBR	180	45.5	94	46	30.9	6.9	2.1	17.9

*j is fire test age

Table 4 shows that for DR samples, the compressive strength at 28 days reduces as the replacement rate increases, as seen in previous works [34]. With the direct replacement of 100 % of RCA, the compressive strength reduced 22.7 % of the initial strength (concrete with NA). In the case of SBR mixes, both studied mixes (40-SBR and 100-SBR) achieved the proposed objectives: at 28 days, compressive strength was approximately the same as concrete made with NA.

2.3. Fire tests

2.3.1. Test setup

The spalling behaviour was evaluated by testing 39 concrete prisms subjected to a standard fire and uniaxial mechanical loading. With the exception of the 10 % replacement rate, six prisms were evaluated for each mix. From these six samples, two load levels were evaluated: 2.5 and 5 MPa. Two days before the spalling tests, the four lateral sides (20 x 10 cm) of the prisms were sealed with aluminium foil tape, which was glued using refractory glue resistant up to 1200 °C. In addition, before the tests the samples were insulated with 12 cm of rock wool from both sides. The combination of aluminium foil and rock wool was used to provide quasi-unidirectional transport of heat and moisture.

An intermediate-scale furnace powered by a linear propane gas burner was used for heating. This furnace was used in similar experimental studies [35–37]. The gas pressure was controlled during the test according to the ISO 834-1:1999 [21]/NF EN 1363-1:2020 [38] fire curve. The furnace has an opening of 20 x 20 cm. Three type K jacketed thermocouples were used to measure the heating curve; they were placed in front of the furnace 1 cm from the heated face of the sample. The thermocouples were placed at heights of 4, 10, and 16 cm from the bottom of the furnace opening. The details of the furnace are shown in Fig.1.

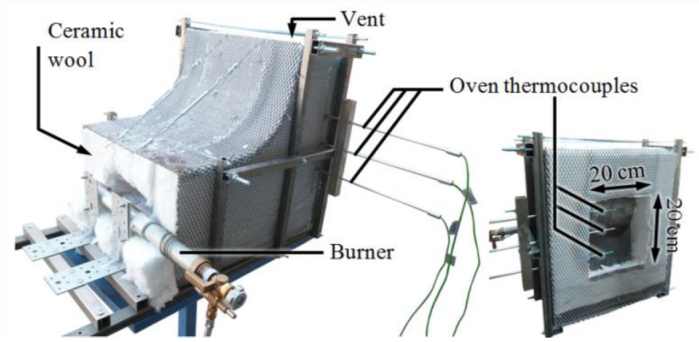

Fig. 1: Furnace details

A hydraulic press was used to apply the uniaxial loading. To ensure the load distribution, the tested specimen was placed between two concrete blocks (top and bottom supports). The sides of the tested specimen and

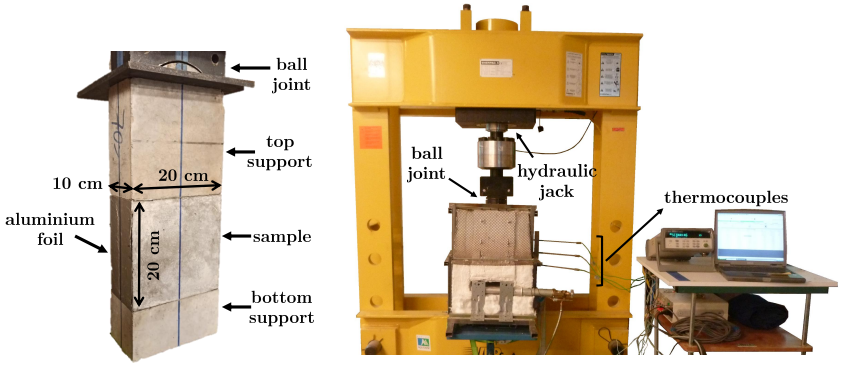

(a) sample and supports (b) furnace and press

Fig. 2: Overview of test setup

support blocks were insulated with rock wool, as well as the hydraulic jack. Some details of the test setup and sample positions are shown in Fig.2. The load was applied first. After stabilisation, the heating process was initiated. After 30 min, the heating was turned off, and, after another 5 min, the sample was discharged. The spalling events were registered using the noises heard during each test. The time of each explosion (or popping) was noted and associated with the occurrence of spalling.

Fig. 3 presents the time-temperature curves from all fire tests. Fig. 3a presents the average of the three thermocouples for each test. The x marks indicate the time of the first spalling event for each sample. Based on these curves, an error evaluation was performed according to NF EN 1363-1:2020 [38] (Fig. 3b). Most of the curves, up to the first spalling event, closely followed the ISO 834-1:1999 [21]/NF EN 1363-1:2020 [38] prescription. After the first spalling time, perturbations were observed at the recorded temperatures. The main criterion adopted for test validation was whether the curve followed the tolerances up to the first spalling event. As Fig. 3b shows, only two fire tests did not consider the tolerance (RCA-10-DR and RCA-20-DR). These two tests were excluded from further analysis.

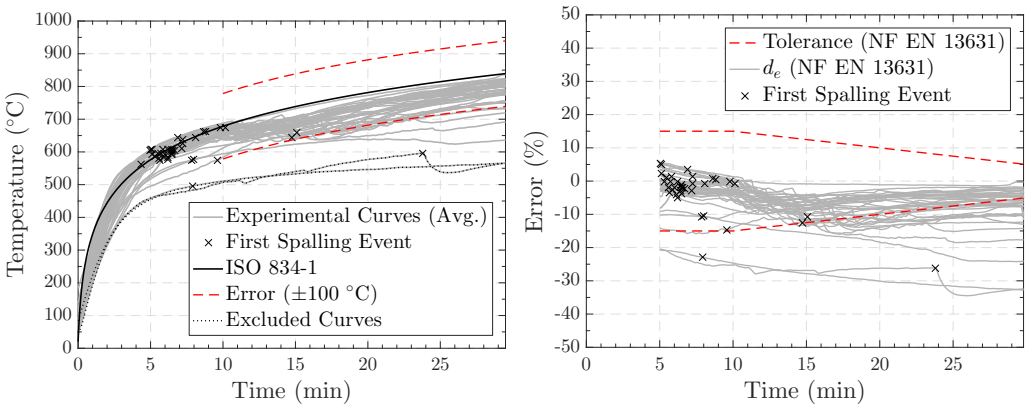

(a) fire curves

(b) error evaluation

Fig. 3: Developed fire curves

2.3.2. Postfire analysis

After heating, a postfire analysis was conducted on all samples. First, mass measurements were performed before and after the fire tests. Digital photogrammetry was then used to quantify the spalling (volume and depth). This method makes it possible to construct 3D models from digital photographs. It has been previously used for different *in situ* and laboratory measurements [39, 40]. This method follows an approach that involves image acquisition and processing, 3D reconstruction, mesh generation, and post-processing [40].

A digital single-lens mirrorless camera (Panasonic DMC-GX80) with a zoom lens (G Vario 14-42 mm f/3.5-5.6 ASPH) was used. This camera has a sensor of 17.3 x 13.3 mm and resolution of 16 megapixels. For image acquisition, the samples were placed in a rotating table with marks on the surface to orient the 3D reconstruction. The camera was fixed on a tripod, and photographs were taken with ISO 400, an aperture of f/14, and a shutter speed of 1/3 seconds. These settings were selected to have an appropriate exposure with a larger depth of field such that all the exposed surfaces of the sample were in focus. Between shots, the rotating table was turned 10° to overlap consecutive images, which is a necessary procedure for 3D reconstruction. Thirty-six images were obtained for each sample; an example of the image taken is shown in Fig.4a.

The image processing and 3D reconstruction were done with Meshroom [41] software. The 3D model of each model was processed using CloudCom-

pare software [42]. Using this software, the 3D model was cleaned and scaled utilizing the reference marks on the rotating table. Fig.4b presents an example of a cleaned and scaled 3D model. A binary mesh of the 3D model was imported in a Cast3m [43] algorithm, which postprocessed the model to obtain the spalling volume and depths. A depth colour map generated in Cast3m [43] is presented in Fig.4c.

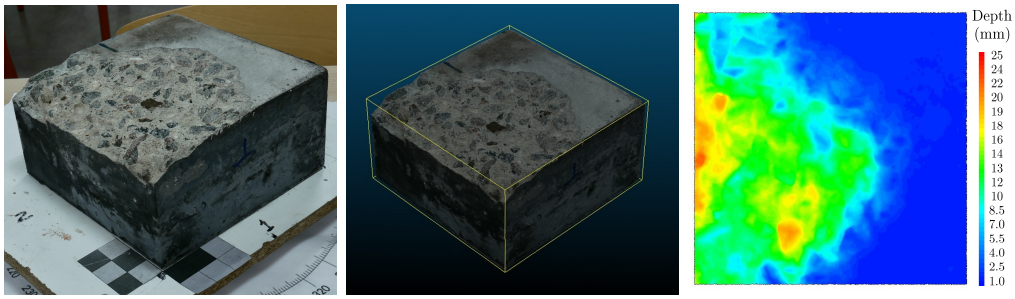

(a) digital photograph (b) 3D model (c) depth colour map

Fig. 4: Steps in the photogrammetry analysis

An accuracy assessment was performed to estimate the error in the photogrammetry measurements. The experiment was conducted using small pieces of (Lego® pieces). A Lego® piece was placed on the surface of a concrete sample, and photogrammetry analysis was performed with this configuration. From this analysis, the dimensions of the Lego® pieces were measured, and the values were compared with the dimensions obtained using a calliper. The difference between the dimensions measured by photogrammetry analysis and the caliper range from 1.06 % to 2.07 %, showing good agreement between the measurements in all experiments. In addition, the results are within the range of different experimental programs that used digital photogrammetry methods (0.11 to 8.63 %) [39, 40].

Table 5: Accuracy assessment of photogrammetry measurements

Lego® Dimension	Calliper	3D Model	Difference (%)
Height (mm)	17.68	17.87	1.06
Width (mm)	15.78	15.55	1.50
Length (mm)	31.8	31.16	2.07

3. Results

3.1. Spalling events during fire tests

Each spalling event was identified through the noises heard during the test. Fig. 5a shows the time of the first spalling event for all the tests (each point indicates one test). Except for one test on RCA-10-DR and one on RCA-100-SBR, the first spalling event occurred between 5 and 10 min. In general, no specific relationship was observed between the time of the first event and load or replacement rate. This range of time to the first spalling falls within the range observed in previous tests [7, 44, 45]. Fig. 5b shows the total number of spalling events for each test. This number of spalling events is correspondent to the number of noises (explosions and poppings) heard during each test. No clear relationship was observed. The data were highly scattered, highlighting the random nature of the spalling phenomenon [46].

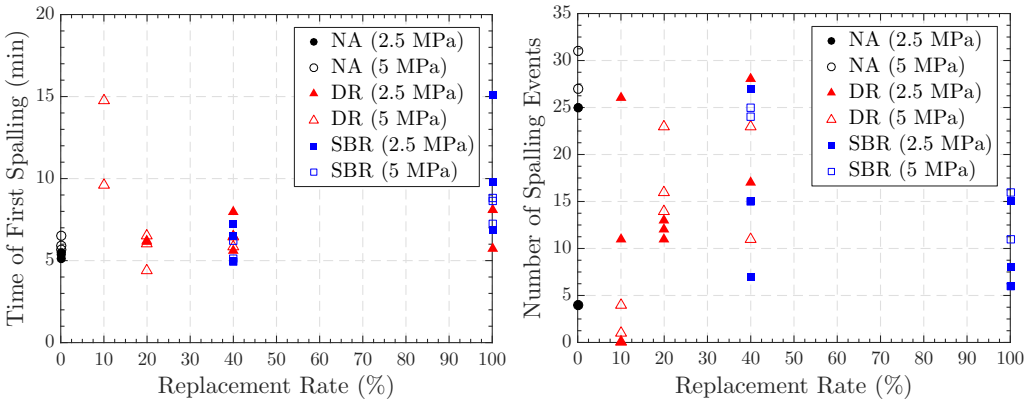

(a) time to first spalling

(b) total spalling events

Fig. 5: Spalling events

3.2. Inspection of samples after fire tests

Based on visual inspection, NA mixes showed less spalling than RCA mixes, regardless of RCA content, compressive strength, or applied load. As an example, Fig. 6 shows four samples after the fire test, together with the depth colour maps generated by the photogrammetry process. The NA mixes almost did not spall, with only some localised spalling. With 20 % RCA (RCA-20-DR), the concrete already had a higher degree of spalling than NA. Finally, both 100 % replacement rate mixes (RCA-100-DR and

RCA-100-SBR) had the highest spalling degree, with no significant visual difference between them.

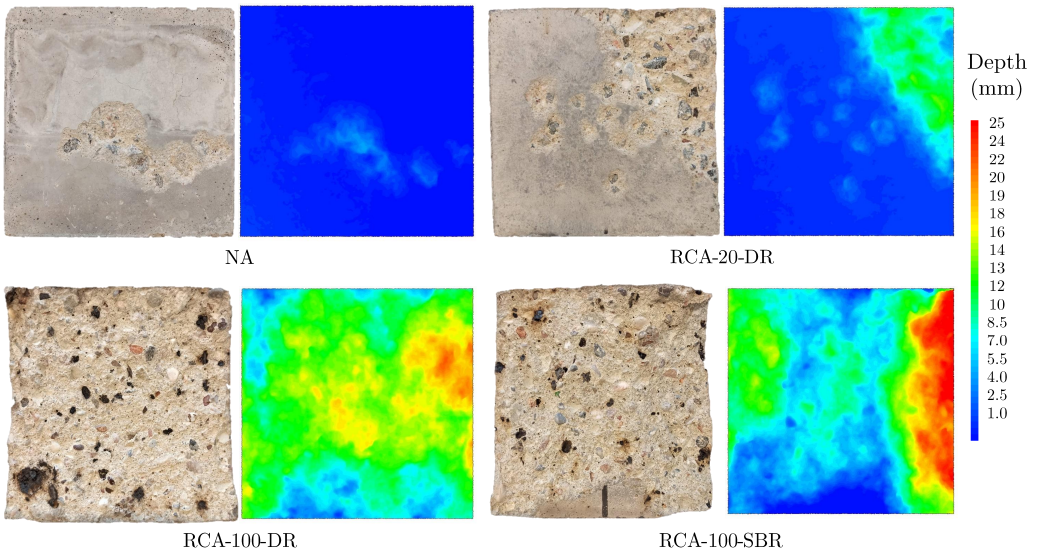

Fig. 6: Four samples after fire test and spalling depths maps

The samples with a high replacement rate presented some burned impurities, mainly bituminous products. Fig. 7a shows that the area around the bituminous particle is black, denoting the burning and melting of this kind of particle. Fig.7b presents a zoom-in of these particles, where it can be seen that the aggregates remain, but the bituminous material disintegrated. The presence of these impurities locally reduced the strength of concrete made with RCA at high temperatures, as observed by Laneyrie et al. [47]. However, it was not possible to establish a link between spalling and impurities in recycled aggregates.

(a) global view (b) zoom-in on a burned impurity

Fig. 7: RCA-40-DR sample after fire test

3.3. Postfire assessment of spalling

The postfire assessment of spalling was performed using four different indicators: total weight loss of the sample (percentage of the initial mass of the sample), spalled volume (percentage of the initial volume of the sample), mean spalling depth (mm) and maximum spalling depth (mm). The last three were obtained using photogrammetry. Fig.8 shows some of the relationships between these indicators (each point is related to a different spalling test). Because the spalled volume is the integral of the mean spalling depth, the relationship these two indicators is not presented.

First, the relationship between the spalled volume and maximum spalling depth is presented at the top left. This relationship relatively linear, with a strong correlation between both indicators, even though they are not directly linked. At the top right, weight loss and spalled volume show a strong correlation. The linearity is expected because a higher spalled volume indicates higher mass loss. Some differences may be associated with the fact that weight loss comprises both the spalled volume and loss resulting from water evaporation. Finally, at the bottom left, the weight loss is compared with the maximum spalling depth. The correlation is lower because a higher maximum spalling depth does not always mean a higher weight loss. Considering all the relationships between the indicators, further analysis will be performed by considering only the spalled volume and maximum spalling depth.

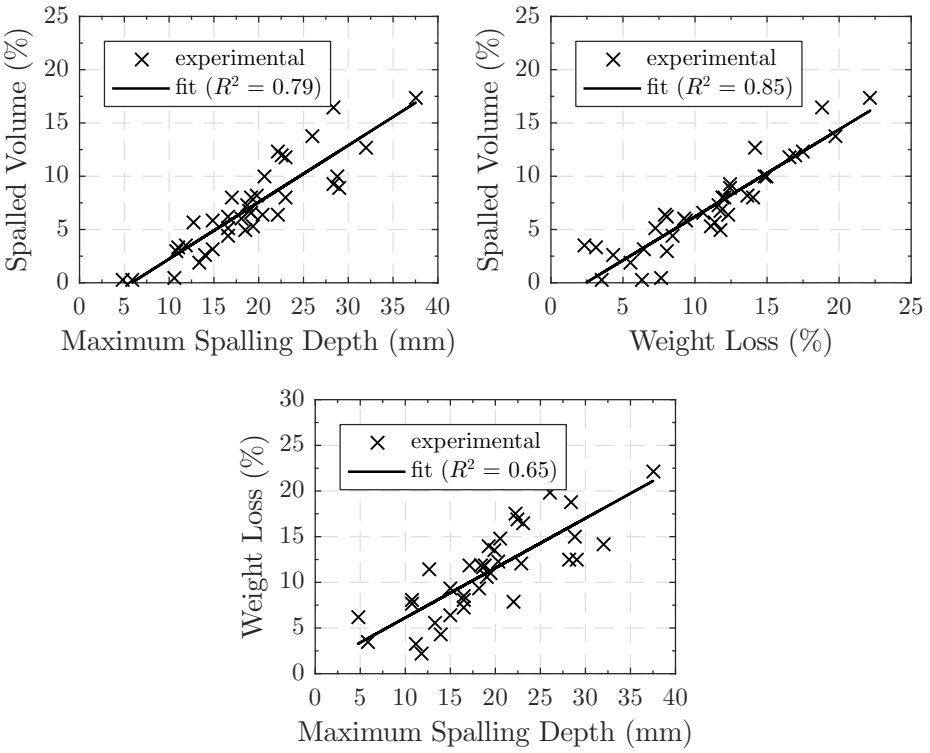

Fig. 8: Relation between spalling indicators

3.3.1. Effect of uniaxial loading during fire test

The effect of uniaxial loading on the fire spalling behaviour is presented in Fig.9, both in terms of the spalled volume (Fig.9a) and maximum spalling depth (Fig.9b). The graphs show each of the mixes analysed with both applied mechanical loads. The bar chart indicates the average value of each spalling indicator, and the error bar shows the scattering of the data. Even though the variation in the individual tests was high, both results indicate that the increase in the loading level led to an increase in spalling, except for RCA-100-DR. Scattering was more significant for concrete made with RCA than for concrete made with NA. However, no direct link to the replacement rate was identified.

The effect of loading was particularly observed for the RCA-40-DR mix, which presented more than twice the spalled volume with a load increase of 3.5 % for 2.5 MPa and 10.1 % for 5 MPa. By contrast, the lowest difference was observed for concrete made with NA, with spalled volumes of 2.05 % and

2.90 % for loadings of 2.5 MPa and 5 MPa, respectively. An increase in the spalled volume with the load was not observed for the RCA-100-DR mix, presenting a higher spalled volume of 2.5 MPa. This was one of the mixes that presented a higher dispersion of results.

Similar observations were made regarding the maximum spalling depth but with an even less clear tendency between the load and spalling depth. For example, NA, RCA-40-SBR, and RCA-100-SBR presented, had the same maximum spalling depth (average value), regardless of the applied load. The largest difference was observed for RCA-40-DR, with a variation of 9 mm between the two loads. In the case of the spalled volume, the RCA-100-DR mix also had a higher maximum spalling depth with a loading of 2.5 MPa.

The key influence of the load on spalling was previously verified in different experimental setups and concrete mixes [48, 49]. However, only a few studies [35, 50, 51] have evaluated the effect of different load levels on concrete. All of this previous studies were made in concrete made with NA. In general, their conclusions agree with the general behaviour observed herein: spalling severity may increase with external load.

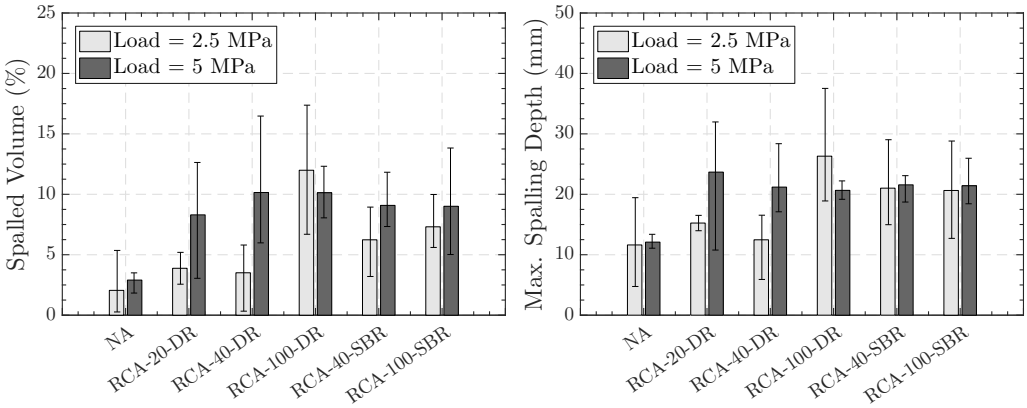

(a) spalled Volume (b) maximum Spalling Depth

Fig. 9: effect of compressive axial loading on spalling indicators

3.3.2. Effect of replacement rate

Figs. 10 and 11 show the effect of replacement rate and the replacement method (DR/SBR) on the spalling behaviour. In these graphs, the scatter points represent the spalling indicator obtained from the postfire analysis of each sample, while the line indicates the average value of this indicator. Spalling indicators (volume and depth) are plotted against the replacement

rate. The data are scattered, highlightingthe random nature of spalling. However, some trends can be verified. As observed in the visual inspection, concrete made with RCA exhibited a higher spalling degree than that made with NA. The spalled volume showed a similar behaviour in most cases: an increase up to a certain replacement rate, followed by a constant value. This was more evident in the DR and SBR samples subjected to 5 MPa. In these curves, the spalled volume increases as the replacement rate increases from 0 % to 40 %. Then, from 40 % to 100 % of the replacement rate, the spalling indicators remain relatively constant, approximately 10 % of the volume loss for DR and 9 % for SBR.

Concerning the replacement method, results show that both type of mixes presented a similar spalling risk. The replacement method affects the cement paste volume and, consequently, the concrete compressive strength. The SBR mixes were designed to have denser and stronger pastes and a higher quantity of cement paste. However, these modifications only slightly affect the general behaviour of the spalled volume. For 2.5 MPa, mixes with 100 % RCA showed higher differences between DR and SBR. The spalled volume in RCA-100-DR was around 5 % higher than RCA-100-SBR. For 5 MPa, DR still presents a higher spalled volume, but the difference is less significant - around 1 %.

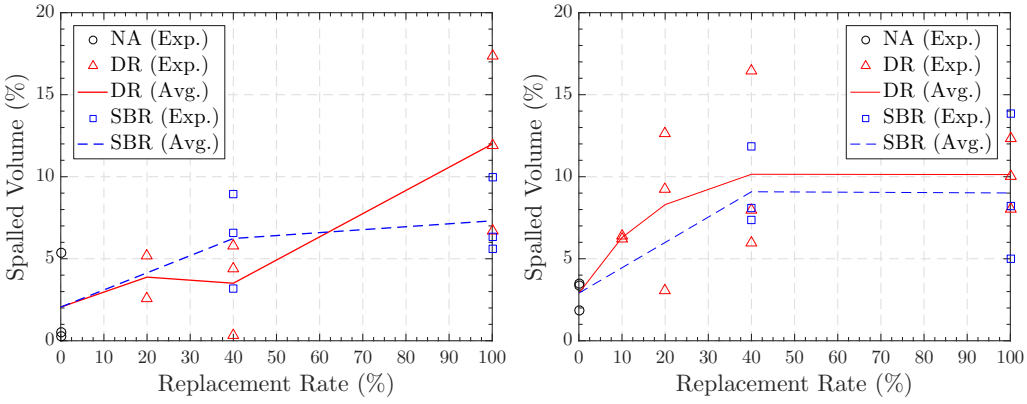

(a) 2.5 MPa (b) 5 MPa

Fig. 10: Effect of replacement on the spalled volume

The evolution of the maximum spalling depth with the replacement rate exhibited the same general trend. However, differences were observed with the DR mixes subjected to a loading of 5 MPa. For these mixes, a higher

maximum spalling depth (23.7 mm) was observed at a replacement rate of 20 %. However, for replacement rates from 40 % to 100 %, the values also remained comparatively constant, from 21.2 mm to 20.7 mm, respectively. This behaviour reinforces the fact that the RCA replacement rate does not change the spalling degree after a certain percentage (after 40 % in this study).

For the effect of replacement methods, similar trends as the ones observed in spalled volume were verified. For 2.5 MPa, higher differences in max spalling depth between DR and SBR. For 100 %, the difference in depth was around 6 mm. In the case of the fire tests with 5 MPa of uniaxial load, the differences become negligible - less than 1 mm between replacement methods. Furthermore, the behaviour observed Figs. 10 and 11 highlight that the replacement method (DR or SBR) did not substantially change the spalling behaviour of concrete made with RCA.

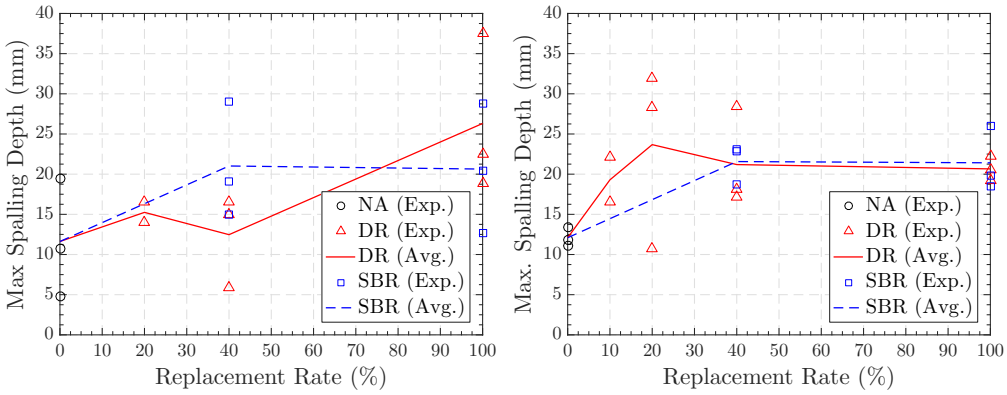

(a) 2.5 MPa (b) 5 MPa

Fig. 11: Effect of replacement on the maximum spalling depth

4. Discussion of the influence of RCA on fire spalling mechanisms in concrete

The general trend observed in the spalled volume and maximum spalling depth indicates that the replacement rate has a contradictory effect on the spalling behaviour. First, up to a 40 % of replacement rate, the spalling degree increased with the presence of RCA. Further addition of RCA did not substantially change the spalling severity. After a replacement level threshold, the presence of RCA kept the spalling degree constant. However, the replacement rate influences several physical properties of concrete that usu-

ally play a crucial role in spalling sensitivity. Two of these, compressive strength and water content, are discussed in this section.

Usually, high compressive strength leads to high compacity and low permeability [2, 52]. These properties may induce the build-up of pore pressure, possibly increasing the spalling risk according to different studies [2, 53]. Fig.12 shows the spalling results against the average compressive strength measured at the test age for each of the studied mixes (each point represents the result of a single fire test). Even if the results are slightly scattered, one can observe that both the spalled volume and the maximum spalling depth tend to decrease as the compressive strength increases. Hence, the trend of spalling risk increasing as the compressive strength increases was not identified for the studied mixes. One mix (RCA-100-DR), which presented a higher average spalled volume (12.0 %) and depth (26.3 mm), had a lower compressive strength. This behaviour indicates that, in this experimental evaluation, compressive strength does not seem to be a factor affecting spalling depth.

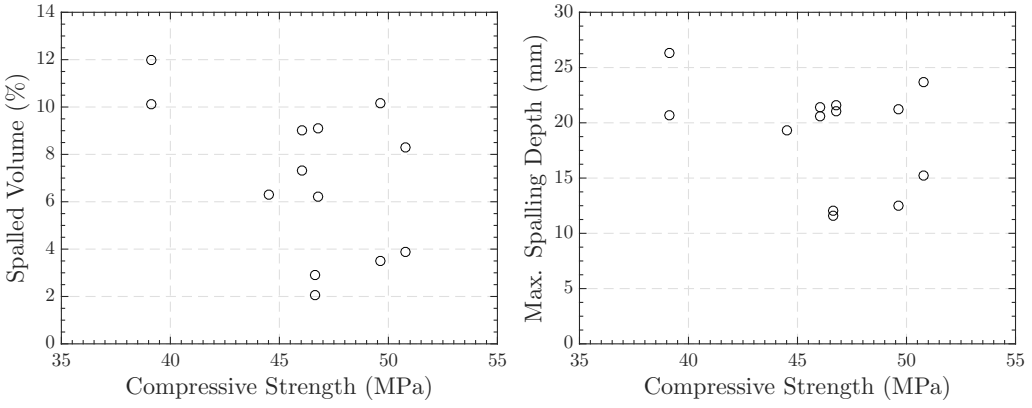

(a) spalled volume (b) maximum spalling depth

Fig. 12: Effect of compressive strength on spalling indicators

The effect of water content on concrete spalling is also related to the build-up of pore pressure [53] and, according to some researchers, can have play a major role in the mechanical properties of concrete at high temperatures [54]. For both cases, and as observed in numerous experimental studies [4, 53, 55], spalling risk is concluded to be higher for high water content.

Fig.13 presents the spalling results against the water content (measured at the test age) for each studied mix (again, scatter points represent the result of each fire test). In the present study, the highest average spalled volume

(12.0 %) and depth (26.3 mm) were observed for the mix with the higher water content (RCA-100-DR, wc=7.6 %), agreeing with the tendency reported in the literature. The results also indicated that spalling is very sensitive to water content. For example, between 5.2 % (NA) and 6.1 % (RCA-40-SBR) water content, the spalled volume increased more than three times (under a mechanical load of 5 MPa). This type of sensitivity was also identified by Maier et al. [18], who verified a higher increase in damage within a small range of initial water content. At the same time, the results presented herein show some cases where the difference in water content was relatively high (6.1 % for RCA-40-SBR and 7.3 % for RCA-100-SBR). However, the maximum spalling depths were quite similar (21.6 mm and 24.4 mm, respectively). After 6.1 %, the spalling parameters remained almost constant.

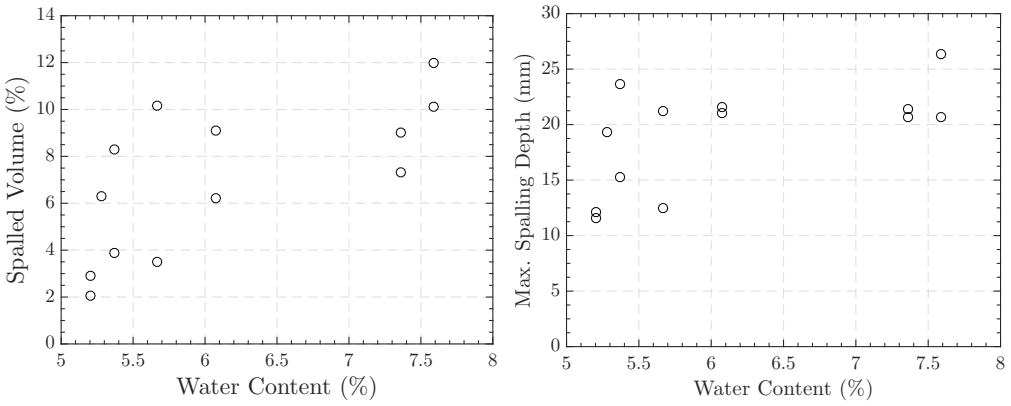

(a) spalled volume (b) maximum spalling depth

Fig. 13: Effect of water content on spalling indicators

In short, compressive strength did not seem to affect the risk of spalling, and the water content appears to be a critical parameter. A higher RCA replacement rate leads to higher water content and spalling risk. However, its effect is insufficient to explain why the extent of spalling of the concrete made with RCA did not evolve from a replacement rate threshold of 40 % in this study. This particular behaviour of concrete made with RCA concerning the risk of spalling should involve other phenomena.

Two hypotheses are highlighted. The first one is related to a lower thermal mismatch between aggregate and paste. For concrete made with RCA, the higher the replacement rate, the more the old-paste–new-paste interfaces become the majority of the paste–aggregate interfaces. Consequently, in-

creasing the replacement rate may decrease the thermal mismatch, leading to a lower cracking density. This reduction may improve the local mechanical properties of the concrete (mainly in the vicinity of the heated surfaces) . For example, this can be observed by comparing the mechanical properties of concretes where the thermal mismatch is different (e.g., concrete made with different aggregates [56, 57]). Finally, this improvement can reduce the risk of spalling in contrast to the previous effect.

The second theory is related to cracking. As verified experimentally in previous works [16], the use of saturated/wet RCA may lead to an excess of water surrounding aggregates. This extra water may reduce the bond in interfaces, inducing cracks and increasing permeability. In addition, the higher initial porosity of RCA also may cause higher permeability in the concrete mixes. This increase in permeability can favour the transport of fluids (liquid water and vapour) in the sensitive spalling zone, decreasing the pore pressure and the risk of spalling.

These effects, which may happen jointly, are some of the phenomena that could explain the results of this study. First, up to a certain replacement rate threshold (40 % in this study), the increase in spalling risk can be explained by the increase in water content. Above this threshold, the highlighted phenomena can counterbalance the effect of the water content and stabilise the spalling characteristics. Further analysis of permeability and microscopic observations of thermal cracking could help to clarify this point.

5. Conclusions

The spalling behaviour of concrete made with recycled concrete aggregates was investigated experimentally. Based on the results, the following conclusions were drawn:

- Digital photogrammetry shows potential for postfire assessment. All spalling measurements showed a good relationship and can serve as appropriate indicators of the degree of damage when assessing the fire risk susceptibility of concrete mixes.

- In general, concrete made with RCA exhibited a higher spalling degree than concrete made with NA. An increase in the compressive axial load led to a slight increase in the spalling degree. Concerning the replacement rate, spalling indicators (volume and maximum depth)

exhibited peculiar behaviour. First, the spalling volume and depth increased from 0 % to 40 %. From 40 % to 100 %, the spalling indicators remained constant. The replacement method (direct replacement or strength-based replacement) did not substantially change the general behaviour.

- The presence of RCA affects different properties that may influence spalling risks, such as the water content and compressive strength. Compressive strength did not affect the spalling risk of concrete made with RCA because concrete mixes with relatively low strength presented a noticeably higher spalling. The water content influenced the spalling damage because mixing with high water content resulted in higher spalling depths and volumes.

- Different hypotheses were proposed about the effect of replacement rate on spalling risk. The increase in spalling risk could be associated with higher water content and lower thermal cracking. At the same time, the possible reduction of spalling risk could be related to the cracking behaviour and the improvement of the mechanical properties of the concrete owing to the lower thermal mismatch.

Finally, it is essential to emphasise that these conclusions are drawn based on the material screening campaign for a specific type of aggregate (for both NA and RCA), from a specific region, with specific properties and nature. Full-scale fire tests on structural elements should be performed to analyse the spalling risk of concrete made with RCA and to verify the influence of possible spalling damage on structural performance (fire resistance).

Acknowledgements

The authors would like to thank Région Nouvelle-Aquitaine for funding (project RECYFEU). They also would like to thank Groupe Cassous (Guyenne Environnement and AQIO) and Groupe Garandeau for their support.

References

[1] G. A. Khoury, Effect of fire on concrete and concrete structures, Progress in Structural Engineering and Materials 2 (2000) 429–447. URL: http://doi.wiley.com/10.1002/pse.51. doi:10.1061/41016(314)299.

[2] J.-C. Liu, K. H. Tan, Y. Yao, A new perspective on nature of fire-induced spalling in concrete, Construction and Building Materials 184 (2018) 581–590. doi:10.1016/j.conbuildmat.2018.06.204.

[3] J. C. Mindeguia, P. Pimienta, A. Noumowé, M. Kanema, Temperature, pore pressure and mass variation of concrete subjected to high temperature - Experimental and numerical discussion on spalling risk, Cement and Concrete Research 40 (2010) 477–487. doi:10.1016/j.cemconres.2009.10.011.

[4] J.-C. Mindeguia, H. Carré, P. Pimienta, C. La Borderie, Experimental discussion on the mechanisms behind the fire spalling of concrete, Fire and Materials 39 (2014) 619–635. doi:10.1002/fam.2254.

[5] B. Lottman, A. Snel, F. Kaalberg, C. Blom, E. Koenders, Spalling mechanism: Key for structural fire resistance of tunnels, Structural Engineering International 31 (2021) 233–240. doi:10.1080/10168664.2020.1796556.

[6] F. L. Monte, R. Felicetti, C. Rossino, Fire spalling sensitivity of high-performance concrete in heated slabs under biaxial compressive loading, Materials and Structures 52 (2019) 1–11.

[7] N. Hua, A. Tessari, N. E. Khorasani, Characterizing damage to a concrete liner during a tunnel fire, Tunnelling and Underground Space Technology incorporating Trenchless Technology Research 109 (2021) 103761. URL: https://doi.org/10.1016/j.tust.2020.103761. doi:10.1016/j.tust.2020.103761.

[8] E. W. H. Klingsch, Explosive spalling of concrete in fire, Ph.D. thesis, ETH Zurich, 2014.

[9] G. Shorter, T. Harmathy, Discussion on the fire resistance of prestressed concrete beams, Proceedings of the Institution of Civil Engineers 20 (1961) 313–315.

[10] T. Harmathy, Effect of moisture on the fire endurance of building elements, in: Moisture in materials in relation to fire tests, ASTM International, 1965, pp. 74–95.

[11] Z. P. Bažant, W. Thonguthai, Pore pressure and drying of concrete at high temperature, Journal of the Engineering Mechanics Division 104 (1978) 1059–1079.

[12] Q. Ma, R. Guo, Z. Zhao, Z. Lin, K. He, Mechanical properties of concrete at high temperature-A review, Construction and Building Materials 93 (2015) 371–383. URL: http://dx.doi.org/10.1016/j.conbuildmat.2015.05.131. doi:10.1016/j.conbuildmat.2015.05.131.

[13] F. Meftah, Pesavento, C. F. Davie, S. Dal Pont, M. Zeiml, M. Korzen, A. Millard, Advanced modelling, in: A. Millard, P. Pimienta (Eds.), Modelling of Concrete Behaviour at High Temperature, Springer, 2019, pp. 27–65.

[14] Z. P. Bažant, W. Thonguthai, Pore pressure in heated concrete walls: theoretical prediction, Magazine of Concrete Research 31 (1979) 67–76.

[15] D. Gawin, C. Majorana, B. Schrefler, Numerical analysis of hygro-thermal behaviour and damage of concrete at high temperature, Mechanics of Cohesive-frictional Materials: An International Journal on Experiments, Modelling and Computation of Materials and Structures 4 (1999) 37–74.

[16] P. Pliya, D. Cree, H. Hajiloo, A.-L. Beaucour, M. Green, A. Noumowé, High-strength concrete containing recycled coarse aggregate subjected to elevated temperatures, Fire Technology (2019) 1–18.

[17] M. Maier, A. Saxer, K. Bergmeister, R. Lackner, An experimental fire-spalling assessment procedure for concrete mixtures, Construction and Building Materials 232 (2020) 117172. URL: https://doi.org/10.1016/j.conbuildmat.2019.117172. doi:10.1016/j.conbuildmat.2019.117172.

[18] M. Maier, M. Zeiml, R. Lackner, On the effect of pore-space properties and water saturation on explosive spalling of fire-loaded concrete, Construction and Building Materials 231 (2020) 117150. doi:10.1016/j.conbuildmat.2019.117150.

[19] B. Fernandes, H. Carré, J.-C. Mindeguia, C. Perlot, C. La Borderie, Effect of elevated temperatures on concrete made with recycled concrete

aggregates-an overview, Journal of Building Engineering (2021) 103235. doi:10.1016/j.jobe.2021.103235.

[20] F. Robert, A.-L. Beaucour, H. Colina, Behavior under fire, in: F. De Larrard, H. Colina (Eds.), Concrete Recycling: Research and Practice, CRC Press, 2019, p. 13.

[21] ISO 834-1, Fire-resistance tests — Elements of building construction — Part 1: General requirements, International Organization for Standardization, Geneva, 1999.

[22] Z. Chen, J. Zhou, P. Ye, Y. Liang, Analysis on Mechanical Properties of Recycled Aggregate Concrete Members after Exposure to High Temperatures, Applied Sciences (2019). doi:10.3390/app9102057.

[23] P. Pliya, H. Hajiloo, S. Romagnosi, D. Cree, S. Sarhat, M. F. Green, The compressive behaviour of natural and recycled aggregate concrete during and after exposure to elevated temperatures, Journal of Building Engineering 38 (2021) 102214. URL: https://doi.org/10.1016/j.jobe.2021.102214. doi:10.1016/j.jobe.2021.102214.

[24] EN 1097-2:2010, Tests for mechanical and physical properties of aggregates. Methods for the determination of resistance to fragmentation, Comité Européen de Normalisation, Brussels, 2010.

[25] EN 1097-6:2013, Tests for mechanical and physical properties of aggregates. Determination of particle density and water absorption, Comité Européen de Normalisation, Brussels, 2013.

[26] EN 933-11, Tests for geometrical properties of aggregates. Classification test for the constituents of coarse recycled aggregate, Comité Européen de Normalisation, Brussels, 2009.

[27] NF EN 206/CN, Béton — Spécification, performance, production et conformité — Complément national à la norme NF EN 206, Comité Européen de Normalisation, Brussels, 2014.

[28] IREX, Comment Recycler Le Béton Dans Le Béton, Institut pour la recherche appliquée et l'expérimentation en génie civil, Paris, 2019.

[29] F. de Larrard, T. Sedran, Betonlab, 2021. URL: https://betonlabpro.ifsttar.fr/.

[30] L. Butler, Evaluation of Recycled Concrete Aggregate Performance in Structural Concrete, Ph.D. thesis, University of Waterloo, 2012.

[31] NF EN 12350-2, Testing fresh concrete - Part 2 : slump test, Comité Européen de Normalisation, Brussels, 2019.

[32] NF EN 12390-7, Essais pour béton durci - Partie 7 : masse volumique du béton durci, Comité Européen de Normalisation, Brussels, 2019.

[33] APC-AFREM, Durabilité des Betons - Méthodes recommandés pour la mesure des granulats associées a la durabilité, Association Française de recherches et d'essais sur les matériaux et constructions, Toulouse, 1997.

[34] R. V. Silva, J. De Brito, R. K. Dhir, The influence of the use of recycled aggregates on the compressive strength of concrete: A review, European Journal of Environmental and Civil Engineering 19 (2014) 825–849. doi:10.1080/19648189.2014.974831.

[35] M. J. Miah, F. Lo Monte, R. Felicetti, H. Carré, P. Pimienta, C. La Borderie, Fire spalling behaviour of concrete: role of mechanical loading (uniaxial and biaxial) and cement type, in: Key Engineering Materials, volume 711, Trans Tech Publ, 2016, pp. 549–555.

[36] M. J. Miah, The Effect of Compressive Loading and Cement Type on the Fire Spalling Behaviour of Concrete, Ph.D. thesis, Université de Pau et des Pays de l'Adour, 2017.

[37] F. Sultangaliyeva, Formulation of fluid fire-resistant fiber-reinforced cementitious composite : Application to radioactive waste disposal, Ph.D. thesis, Université de Pau et des Pays de l'Adour, 2017.

[38] NF EN 1363-1, Essais de résistance au feu - Partie 1 : exigences générales, Comité Européen de Normalisation, Brussels, 2020.

[39] A. E. Kenarsari, S. J. Vitton, J. E. Beard, Creating 3D models of tractor tire footprints using close-range digital photogrammetry, Journal of Terramechanics 74 (2017) 1–11. URL: http://dx.doi.org/10.1016/j.jterra.2017.06.001. doi:10.1016/j.jterra.2017.06.001.

[40] E. Cavaco, R. Pimenta, J. Valença, A new method for corrosion assessment of reinforcing bars based on close-range photogrammetry: Experimental validation, Structural Concrete 20 (2019) 996–1009.

[41] AliceVision, Meshroom: A 3D reconstruction software., 2018. URL: https://github.com/alicevision/meshroom.

[42] G. Software, Cloud compare, 2021. URL: http://www.cloudcompare.org/.

[43] CEA, Cast3m, 2021. URL: http://www-cast3m.cea.fr/.

[44] L. Boström, R. McNamee, J. Albrektsson, P. Johansson, Screening test methods for determination of fire spalling of concrete, Technical Report, RISE, 2018.

[45] S. Mohaine, F. Robert, L. Boström, M. Lion, R. Mcnamee, Cross-comparison of screening tests for fire spalling of concrete, Fire and Materials (2021) 1–14. doi:10.1002/fam.2946.

[46] C. Maluk, L. Bisby, G. P. Terrasi, Effects of polypropylene fibre type and dose on the propensity for heat-induced concrete spalling, Engineering Structures 141 (2017) 584–595.

[47] C. Laneyrie, A.-L. Beaucour, M. F. Green, R. L. Hebert, B. Ledesert, A. Noumowe, Influence of recycled coarse aggregates on normal and high performance concrete subjected to elevated temperatures, Construction and Building Materials 111 (2016) 368–378.

[48] L. Boström, U. Wickström, B. Adl-Zarrabi, Effect of specimen size and loading conditions on spalling of concrete, Fire and Materials: An International Journal 31 (2007) 173–186.

[49] M. Guerrieri, C. Sanabria, W. M. Lee, E. Pazmino, R. Patel, Design of the metro tunnel project tunnel linings for fire testing, Structural Concrete 21 (2020) 2452–2480.

[50] H. Carré, P. Pimienta, C. La Borderie, F. Pereira, J.-C. Mindeguia, Effect of compressive loading on the risk of spalling, in: MATEC Web of Conferences, volume 6, EDP Sciences, 2013, p. 01007.

[51] F. Lo Monte, R. Felicetti, Heated slabs under biaxial compressive loading : a test set-up for the assessment of concrete sensitivity to spalling, Materials and Structures 50 (2017) 1–12. doi:10.1617/s11527-017-1055-1.

[52] V. Kodur, L. Phan, Critical factors governing the fire performance of high strength concrete systems, Fire safety journal 42 (2007) 482–488.

[53] Y. Li, E.-H. Yang, A. Zhou, T. Liu, Pore pressure build-up and explosive spalling in concrete at elevated temperature: A review, Construction and Building Materials 284 (2021) 122818.

[54] R. Jansson, Fire spalling of concrete: theoretical and experimental studies, Ph.D. thesis, KTH Royal Institute of Technology, 2013.

[55] L. T. Phan, Pore pressure and explosive spalling in concrete, Materials and structures 41 (2008) 1623–1632.

[56] J.-C. Mindeguia, P. Pimienta, H. Carré, C. La Borderie, On the influence of aggregate nature on concrete behaviour at high temperature, European Journal of Environmental and Civil Engineering 16 (2012) 236–253. doi:10.1080/19648189.2012.667682.

[57] Z. Xing, A.-L. Beaucour, R. Hebert, A. Noumowe, B. Ledesert, Influence of the nature of aggregates on the behaviour of concrete subjected to elevated temperature, Cement and concrete research 41 (2011) 392–402.